RP Current Trends In Applied Sciences (e-ISSN: 2583-7486)
Vol. 5, No. 2 (April – June 2026) pp. 110–117

Cite this article: S.K. Chanu, W.N. Singh, L.N. Singh, T.R. Singh, H.O. Singh, Analysis of Gravastar model in modified *f*(*R*,*L*$_m$,*T*) gravity, *RP Cur. Tr. Appl. Sci.* **5** (2026) 110–117.

Original Research Article

Analysis of Gravastar model in modified $f(R,L_m,T)$ gravity

Salam Kiranmala Chanu[1,*], Wahengbam Nimai Singh[2] Laishram Nevy Singh[2], Thokchom Revekson Singh[3], Huidrom Open Singh[3]

[1]DM College of Arts, Dhanamanjuri University, Manipur, India
[2]Kamakhya Pemton College, Manipur, India
[3]Research Scholar DM College of Arts, Dhanamanjuri University, Manipur, India
*Corresponding author, E-mail: kiranmala07@gmail.com

ARTICLE HISTORY
Received: 06 May 2026
Revised: 18 June 2026
Accepted: 18 June 2026
Published: 19 June 2026

KEYWORDS
Gravastar; $f(R,L_m,T)$ gravity; Equation of State (EOS); Matter geometry coupling.

ABSTRACT
The Gravastar (Gravitational vacuum star) is considered as viable alternative to Black Holes, avoiding singularity and event horizon through a compact structure composed of a de-Sitter core with $p = -\rho$, a thin shell of ultra relativistic stiff matter with $p = \rho$ and an exterior schwarzchild vacuum region with $p = \rho = 0$. In this paper, modified gravity frameworks are employed in Gravastar modeling to reduce reliance an exotic matter, improve stability, and provide a more fundamental mechanism for singularity avoidance beyond standard General Relativity. We have investigated a Gravastar configuration within the framework of modified gravity theory $f(R,L_m,T)$ gravity using the model $f(R,L_m,T) = R + \lambda_1 L_m + \lambda_2 T$. We have analysed several physical properties of the system including energy density, proper length, total energy and entropy. The vacuum exterior region of the Gravastar is taken to be Scwarzchild de-Sitter exterior solution. And we have also studied junction condition from Darmois-Israel formalism, which are employed to smoothly match the interior and exterior regions leading to well-defined surface stresses at the shell. The results obtained in this paper demonstrate that the inclusion of matter geometry coupling significantly modifies the equilibrium configuration and physical properties of Gravastar providing a viable alternative to black holes within modified gravity.

1. Introduction

The study of the endpoint of gravitational collapse has been the most fundamental and challenging problem in relativistic astrophysics and gravitational physics. Black holes formed by gravitational collapse of massive stars within the framework of General Relativity (GR) leads to the formation of singularities and event horizon which signals as breakdown of classical theory. A Gravastar (gravitational vacuum star), alternative to black holes, introduced by [1], avoids the formation of singularity and event horizon Gravastar is a gravitational collapse cold dark, compact object with an interior de-Sitter condensate phase ($0 \leq r \leq R_1$), a thin shell of stiff matter ($R_1 \leq r \leq R_2$) and an exterior schwarzchild geometry ($R_2 \leq r$) [2]. The event horizon is located at $r = 2M$, referred to as the schwarzchild radius, which defines the boundary of a black Hole, where M represents the total gravitational mass of the black hole. In the interior region of the Gravastar the equation of state $p = \omega\rho$ becomes $p = -\rho(\omega = -1)$, where ρ and p are energy density and pressure respectively. And in the thin shell region equation of state $p = \rho(\omega = 1)$ and in the exterior region with the equation of state $p = \rho = 0$. Many researchers have been interested in the study of Gravastar model in different modified gravitational theories [3,7]. Also researchers have investigated Gravastar model as an alternative black hole theory within the framework General Relativity (GR) [8,10]. But GR has limitations in explaining dark energy, late-time cosmic acceleration [11,15] even though it has been successfully described the large-scale structure and evolution of universe and several phenomena of gravity over a wide range of scales. The researchers have been studying in the modified theories of gravity by changing gravitational sector of Einstein field equations to explain cosmic acceleration.

The modified gravity theories include $f(R)$, $f(T)$, $f(R,T), f(R,L_m), f(R,L_m,T)$ gravity model etc. In $f(R)$ gravity model [16,17], the Einstein Hilbert action is generalized by replacing the Ricci scalar R with an arbitrary function $f(R)$. In $f(R,T)$ theory [18], the gravitational Lagrangian depends on both Ricci scalar R and trace T of the energy-momentum tensor.

The modified gravity $f(R,L_m)$ [19] allows gravitational action to be an arbitrary function of Ricci scalar R and the matter Lagrangian L_m. In modified theory $f(R,L_m,T)$ gravity [20, 21], the gravitational Lagrangian depends not only R but also on L_m and T, thereby unifying $f(R,T)$ and $f(R,L_m)$ gravity theories and providing new gravitational effects beyond GR. This theory leads to non-minimal coupling, non-conservation of energy-momentum tensor and emergence of an extra force making the theory highly suitable for studying compact objects like Gravastar. The effect of changed on Gravastar model in $f(R,T)$ gravity have investigated in [22]. The stable Gravastar model for a particular matter Lagrangian in the foundation of $f(R,L_m,T)$ gravity in the static spherically symmetric space-time have investigated in [23]. In this paper, we consider the $f(R,L_m,T)$ gravity model given by $f(R,L_m,T) = R + \lambda_1 L_m + \lambda_2 T$, where λ_1 and λ_2 are coupling parameters that governs the interaction between matter and geometry. The presence of term $\lambda_1 L_m$ and $\lambda_2 T$ modifies the field equations of GR and leads to non-conservation of energy-momentum tensor which in turn affects the internal structure and physical properties of Gravastar.

The paper is organized as follows: in section 2, we present gravitational field equations in $f(R, L_m, T)$ gravity. In section 3, we obtained cosmological solutions of $f(R, L_m, T)$ gravity model $f(R, L_m, T) = R + \lambda_1 L_m + \lambda_2 T$. In section 4, we analyse the spacetime geometry of Gravastar. Physical characteristics of Gravastar model is investigated in section 5. In section 6, we discuss junction conditions between the interior and extrior regions of Gravastar. Finally, the conclusions are presented in section 7.

2. Gravitational field equations in *f*(*R*,*L*$_m$,*T*) gravity

The Einstein-Hilbert action for $f(R, L_m, T)$ gravity theory with strong geometry-matter coupling is given by

$$S = \int \left[\frac{1}{16\pi} f(R, L_m, T) + L_m\right]\sqrt{-g}\, d^4x \tag{1}$$

where R is the Ricci scalar, L_m is the matter Lagrangian, $T = g^{\mu\vartheta}T_{\mu\vartheta}$ is the trace of the energy momentum tensor and $g = det(g_{\mu\vartheta})$, where $g_{\mu\vartheta}$ is the metric tensor. We assume natural units $C = G = 1$. The energy momentum tensor $T_{\mu\vartheta}$ is defined by

$$T_{\mu\vartheta} = -\frac{2}{\sqrt{-g}}\frac{\delta(\sqrt{-g}L_m)}{\delta g^{\mu\vartheta}} \tag{2}$$

By varying the action (1) with respect to the metric tensor $g_{\mu\vartheta}$ yields the following modified field equations:

$$f_R R_{\mu\vartheta} - \frac{1}{2} f g_{\mu\vartheta} + (g_{\mu\vartheta}\Box - \nabla_\mu\nabla_\vartheta) f_R = 8\pi T_{\mu\vartheta} - f_T(T_{\mu\vartheta} + \theta_{\mu\vartheta}) + \frac{1}{2} f_{L_m}(T_{\mu\vartheta} - L_m g_{\mu\vartheta}) \tag{3}$$

where $f_R = \frac{\partial f}{\partial R}$, $f_T = \frac{\partial f}{\partial T}$, $f_{L_m} = \frac{\partial f}{\partial L_m}$, ∇_μ represents the covariant derivative to symmetric connection $g_{\mu\vartheta}$ and $\Box = \nabla^\mu\nabla_\mu = \frac{1}{\sqrt{-g}}\partial_\mu\sqrt{-g}g^{\mu\vartheta}\partial_\vartheta$ is the d'Alembertion (wave operator).

Here the tensor $\Theta_{\mu\vartheta}$ is defined as:

$$\Theta_{\mu\vartheta} = g^{\alpha\beta}\frac{\delta T_{\alpha\beta}}{\delta g^{\mu\vartheta}} = -2T_{\mu\vartheta} + g_{\mu\vartheta}L_m - 2g^{\alpha\beta}\frac{\partial^2 L_m}{\partial g^{\mu\vartheta}\partial g^{\alpha\beta}} \tag{4}$$

By using the contracted Bianchi identity

$$\nabla^\mu G_{\mu\vartheta} = 0 \tag{5}$$

and the derivative commutative identity

$$\nabla^\mu(g_{\mu\vartheta}\Box f_R - \nabla_\mu\nabla_\vartheta f_R) = -R^\lambda_\vartheta\nabla_\lambda f_R \tag{6}$$

and noting the chain rule

$$\nabla_\vartheta f(R, L_m, T) = f_R\nabla_\vartheta R + f_T\nabla_\vartheta T + f_{L_m}\nabla_\vartheta L_m \tag{7}$$

The covariant divergence of the field equation (3) yields

$$\nabla^\mu T_{\mu\vartheta} = \frac{1}{8\pi - f_T + \frac{1}{2}f_{L_m}}\left[(T_{\mu\vartheta} + \Theta_{\mu\vartheta})\nabla^\mu f_T + \frac{1}{2}(T_{\mu\vartheta} - L_m g_{\mu\vartheta})\nabla^\mu f_{L_m} + f_T\nabla^\mu\Theta_{\mu\vartheta}\right] \tag{8}$$

3. Cosmological solutions for *f*(*R*,*L*$_m$,*T*) gravity

We consider the model

$$f(R, L_m, T) = R + \lambda_1 L_m + \lambda_2 T$$

where λ_1 and λ_2 are arbitrary coupling constants.

Now, we compute $f_R = 1, f_T = \lambda_2, f_{L_m} = \lambda_1, \nabla_\mu f_R = 0, \nabla_\mu f_T = 0$.

Using the above substitutions, equation (3) can be obtained as:

$$G_{\mu\vartheta} = 8\pi T_{\mu\vartheta} - \lambda_2(T_{\mu\vartheta} + \Theta_{\mu\vartheta}) + \lambda_1(T_{\mu\vartheta} - L_m g_{\mu\vartheta}) + \frac{1}{2}(\lambda_1 L_m + \lambda_2 T)g_{\mu\vartheta} \tag{9}$$

and equation (8) becomes

$$\nabla^\mu T_{\mu\vartheta} = \frac{\lambda_2}{8\pi - \lambda_2 + \frac{1}{2}\lambda_1}\nabla^\mu\Theta_{\mu\vartheta} \tag{10}$$

If $\lambda_1 = 0, \lambda_2 = 0$, then

$$G_{\mu\vartheta} = 8\pi T_{\mu\vartheta} \text{ and } \nabla^\mu T_{\mu\vartheta} = 0$$

Which is the GR limit.

Now we consider the spherically symmetric metric

$$ds^2 = e^{\vartheta(r)}dt^2 - e^{\lambda(r)}dr^2 - r^2(d\theta^2 + \sin^2\theta\, d\emptyset^2) \tag{11}$$

where ϑ and λ are two unknown functions of radial co-ordinate r.

The non-zero components of Einstein tensor are given as:

$$G^0_0 = \frac{1}{r^2}(1 - e^{-\lambda}) - \frac{\lambda'}{r}e^{-\lambda} \tag{12}$$

$$G^1_1 = \frac{1}{r^2}(1 - e^{-\lambda}) - \frac{\vartheta'}{r}e^{-\lambda} \tag{13}$$

$$G^2_2 = G^3_3 = \frac{e^{-\lambda}}{4}\left[2\vartheta'' + \vartheta'^2 - \vartheta'\lambda' + \frac{2}{r}(\vartheta' - \lambda')\right] \tag{14}$$

where prime denotes the derivative with respect to the radial co-ordinate r.

We assume that the universe is filled with a matter distribution represented by the energy-momentum tensor of a perfect fluid defined by

$$T_{\mu\vartheta} = (\rho + p)u_\mu u_\vartheta + p g_{\mu\vartheta} \tag{15}$$

where p and ρ are the pressure and energy density of the perfect fluid and u_μ is the four-velocity vector such that $u_\mu u^\mu = -1$.

Denoting $x^0 = 1,\ x^1 = r,\ x^2 = \theta,\ x^3 = \emptyset$ and using co-moving co-ordinates

$$u^\mu = \left(e^{-\frac{\vartheta}{2}}, 0,0,0\right),$$

The non-zero components of the energy momentum tensor of a perfect fluid are

$$T_0^0 = -\rho,\ T_1^1 = T_2^2 = T_3^3 = p \tag{16}$$

For a perfect fluid, we assume $L_m = -\rho$, then from equation (4), we get

$$\Theta_{\mu\vartheta} = \left(-2T_{\mu\vartheta} - \rho g_{\mu\vartheta}\right) \tag{17}$$

Substituting the value of equation (17) in equation (9), we get

$$\mathrm{G}_{\mu\vartheta} = (8\pi + \lambda_1 + \lambda_2)T_{\mu\vartheta} + \left[\rho\left(\lambda_2 + \tfrac{1}{2}\lambda_1\right) + \tfrac{1}{2}\lambda_2\right] g_{\mu\vartheta} \tag{18}$$

Using $T = -\rho + 3p$ in equation (18), we get

$$\mathrm{G}_{\mu\vartheta} = (8\pi + \lambda_1 + \lambda_2)T_{\mu\vartheta} + \left[\rho\left(\lambda_2 + \tfrac{1}{2}\lambda_1\right) + \tfrac{1}{2}\lambda_2(\rho + 3p)\right] g_{\mu\vartheta} \tag{19}$$

By using equations (12), (13), (14) the field equation (19) can be formulated as:

$$\frac{1}{r^2}\left(1 - e^{-\lambda}\right) - \frac{\lambda'}{r}e^{-\lambda} = \rho\left(8\pi + \tfrac{3}{2}\lambda_1 + \tfrac{3}{2}\lambda_2\right) - \tfrac{3}{2}\lambda_2 p \tag{20}$$

$$\frac{1}{r^2}\left(1 - e^{-\lambda}\right) - \frac{\vartheta'}{r}e^{-\lambda} = \rho\left(\tfrac{1}{2}\lambda_1 + \tfrac{3}{2}\lambda_2\right) - p\left(8\pi + \lambda_1 + \tfrac{5}{2}\lambda_2\right) \tag{21}$$

$$\frac{e^{-\lambda}}{4}\left[2\vartheta'' + \vartheta'^2 - \vartheta'\lambda' + \frac{2}{r}(\vartheta' - \lambda')\right] = \rho\left(\tfrac{1}{2}\lambda_1 + \tfrac{3}{2}\lambda_2\right) - p\left(8\pi + \lambda_1 + \tfrac{5}{2}\lambda_2\right) \tag{22}$$

By using equation (17), equation (10) can be written as:

$$\nabla^\mu T_{\mu\vartheta} = -\frac{\lambda_2}{8\pi + \frac{1}{2}\lambda_1 + \lambda_2} g_{\mu\vartheta}\nabla^\mu \rho \tag{23}$$

Using equation (18) and noting $G_1^1 = 8\pi p_{eff}$, we get

$$p_{eff} = p + \frac{1}{16\pi}[\lambda_1\rho + \lambda_2(\rho - 3p)] \tag{24}$$

Using equation (21) and considering the mass function define by $e^{-\lambda} = 1 - \frac{2m(r)}{r}$ and noting $G_1^1 = 8\pi p_{eff}$, we get the relation define by

$$\frac{\vartheta'}{2} = \frac{m(r) + 4\pi r^3 p_{eff}}{r(r - 2m)} \tag{25}$$

By using equation (23) and (25), we get the hydrostatic equilibrium equation for the stellar system with spherically static symmetrical structure in $f(R, L_m, T) = R + \lambda_1 L_m + \lambda_2 T$ model as:

$$\frac{dp}{dr} = \frac{(\rho + p)[m(r) + 4\pi r^3 p_{eff}]}{r(r - 2m)} - \frac{\lambda_2}{8\pi + \frac{1}{2}\lambda_1 + \lambda_2}\frac{d\rho}{dr} \tag{26}$$

For $\lambda_1 = \lambda_2 = 0$, we can reduce it to the standard form of the Tohman-Oppenheimer-Volkoff (TOV) equations as in the case of the GR.

4. Space-time Geometry of Gravastar

Gravastar's structure has three regions namely the interior region $(0 < r < R_1)$, a thin shell of stiff matter $(R_1 < r < R_2)$ and an exterior region $(R_2 < r)$ which resembles the exterior solution discovered by Karl Schwarzchild.

Case I: $\boldsymbol{\omega = -1}$ (Interior region) $(\boldsymbol{0 \le r \le R_1})$

In this case, the equation of state is

$$p = -\rho \tag{27}$$

Using this condition and the non-conservation of the energy momentum tensor, we can have

$$\rho = \rho_k(constant) \tag{28}$$

and thus the pressure becomes

$$p = -\rho_k \tag{29}$$

Under this conditions, equation (20), takes the form

$$e^{-\lambda} = 1 - \frac{\rho_k}{3}\left(8\pi + \frac{3}{2}\lambda_1 + 3\lambda_2\right)r^2 \tag{30}$$

The central active gravitational mass is given by

$$M(R_1) = \int_0^{R_1} 4\pi r^3 \rho_k dr = \frac{4\pi}{3}{R_1}^3\rho_k \tag{31}$$

From figure 1, we see that at $r = 0$, $e^{-\lambda}(0) = 1$ which implies that metric function is clearly regular at $r = 0$ having no Central singularity. As r increases the metric decreases and at some radius $r = R_1$, $e^{-\lambda}(R_1) = 1$, which defines the boundary of the interior region.

Case II: $\omega = 1$ (Shell region) $(R_1 < r \leq R_2)$

The matter distribution in this shell region is assumed to consists of an ultrarelativistic stiff fluid obeying the equation of state $p = \rho$.

The shell contains finite stiff fluid coupled to the cold baryonic matter [24]. In the shell region, we assume that the metric potential satisfies $0 < e^{-\lambda} << 1$ indicating that the spacetime is highly compact. Under this thin shell approximation, we have $1 - e^{-\lambda} \approx 1$.

Neglecting higher-order in metric variations under the thin shell approximation, where metric functions vary slowly and adopting the stiff fluid equation of state $p = \rho$, the field equations (20) – (22) reduce in the following simplified form

$$\frac{1}{r^2} - \frac{\lambda'}{r}e^{-\lambda} = \rho\left(8\pi + \frac{3}{2}\lambda_1\right) \tag{32}$$

$$\frac{1}{r^2} + \frac{\vartheta'}{r}e^{-\lambda} = \rho\left(8\pi + \frac{1}{2}\lambda_1 + \lambda_2\right) \tag{33}$$

$$\frac{e^{-\lambda}}{2r}(\vartheta' - \lambda') = -\rho\left(8\pi + \frac{1}{2}\lambda_1 + \lambda_2\right) \tag{34}$$

Solving these equations (32) – (34), we get

$$e^{-\lambda} = C - \ln r + \frac{\rho}{2}\left(8\pi + \frac{3}{2}\lambda_2\right)r^2 \tag{35}$$

where C is the constant of integration, where $R_1 < r < R_2$ and we assume $R_2 - R_1 = \epsilon$, where $\epsilon \ll 1$ (very small quantity) and $R \sim 1$ (radius of configuration).

Substituting the condition $p = \rho$ in equation [24] and [26] assuming in the Gravastar shell $m(r) \approx M = constant$, we get

$$p(r) = \rho(r) = -\frac{1}{4\pi\beta r^3}W\left[-4\pi\beta r^3\epsilon\left(\frac{r}{r-2M}\right)^{\frac{1}{1+k}}\right] \tag{36}$$

where

$$\beta = 1 + \frac{1}{16\pi}(\lambda_1 - 2\lambda_2)$$
$$k = \frac{\lambda_2}{8\pi + \frac{1}{2}\lambda_1 + \lambda_2}$$

where W is Lambert function.

From equation (26), we notice that pressure p depends on the radial co-ordinate due to matter-geometry coupling.

Case III: $\omega = 0$ (Exterior region) $(R_2 < r)$

The exterior vacuum space-time of Gravastar is described by the equation of state

$$p = \rho = 0 \tag{37}$$

The exterior spacetime resembles the exterior solution discovered by Karl Schwarzchild which is given by

$$ds^2 = \left(1 - \frac{2M}{r}\right)dt^2 - \left(1 - \frac{2M}{r}\right)dr^2 - r^2(d\theta^2 + \sin^2\theta d\emptyset^2) \tag{38}$$

where M being the mass of the gravitational system.

5. Physical characteristics of the Gravastar model

A. Proper length of the shell

The stiff matter shell layer which acts as a stabilizing layer separating the radius of the inner boundary of the shell of the Gravastar i.e. $r = R_1$ and radius of the outer parameter of the shell $R_2 = R_1 + \epsilon$, where ϵ, which indicates the proper shell thickness. We assume $R \sim 1$ (radius of the configuration) and $e << 1$, which is very small. The proper length of the shell region is given by

$$l = \int_{R_1}^{R_1+\epsilon}\sqrt{e^{\lambda}}dr = \int_{R_1}^{R_1+\epsilon}\frac{dr}{\sqrt{C - \ln r + \frac{\rho}{2}\left(8\pi + \frac{3}{2}\lambda_1\right)r^2}} \tag{39}$$

Integrating equation (39), we get

$$l = \frac{\epsilon}{\sqrt{C - \ln R_1 + \frac{\rho}{2}\left(8\pi + \frac{3}{2}\lambda_1\right){R_1}^2}} \tag{40}$$

From equation (40), we observe that the proper thickness of the shell depends inversely on the metric potential and is controlled by the coupling parameter λ_1, while λ_2 term does not contribute in the stiff fluid shell region. The shell becomes thinner if $\lambda_1 > 0$ and it becomes thicker if $\lambda_1 < 0$.

B. Energy content

The interior region of the Gravastar contain finite vacuum energy which acts as a repulsive nature avoiding singularity. Thus the energy content within the shell region of Gravastar is given by

$$E = \int_{R_1}^{R_1+\epsilon} 4\pi\rho r^2\, dr \tag{41}$$

where $p(r) = \rho(r) = -\frac{1}{4\pi\beta r^3}W\left[-4\pi\beta r^3 C\left(\frac{r}{r-2M}\right)^{\frac{1}{1+k}}\right]$

C. Entropy within the shell region

Total entropy of the Gravastar is mainly concentrated in the shell region and there is no entropy in the core (interior) region [1,2].

By using equation (11), the entropy can be measured as

$$S = 4\pi\int_{R_1}^{R_1+\epsilon} S(\pi)r^2\sqrt{e^{\lambda}}dr \tag{42}$$

where $S(r)$ denotes local entropy density at a given temperature $T(r)$ and

$$S(r) = \frac{\sigma^2 {k_B}^2 T(r)}{4\pi h^2} = \gamma\left(\frac{k_B}{h}\right)\sqrt{\frac{p}{2\pi}} \tag{43}$$

where γ is a dimensionless parameter, k_B is Boltzmann constant, h is plank constant.

Substituting equation (43) into equation (42)

$$S = \int_{R_1}^{R_1+\epsilon} 4\pi r^2 \gamma\left(\frac{k_B}{h}\right)\sqrt{\frac{p}{2\pi}}\sqrt{e^{\lambda}}dr \tag{44}$$

where $e^{\lambda} = \frac{1}{C - \ln r + \frac{\rho}{2}\left(8\pi + \frac{3}{2}\lambda_1\right)r^2}$

and

$$\omega = \rho(r) = p(r) = -\frac{1}{4\pi\beta r^3} W\left[-4\pi\beta r^3 C\left(\frac{r}{r-2M}\right)^{\frac{1}{1+k}}\right]$$

6. Junction condition between the interior and the exterior of Gavastar

According to Darmois-Israel formalism [25, 26], the interior de-Sitter spacetime and exterior Scwarzchild geometry are smoothly matched across a thin shell Isreal junction condition. The thin shell Gravastar Characterised by a stiff fluid with equation of state $p = \rho$ supports non-zero energy density and pressure, ensuring the stability of Gravastar configuration.

At the junction surface, the stress energy tensor according to Lanczos equation [38, 39] is given as

$$S_{ij} = \frac{1}{8\pi}\left(k_{ij} - \delta_{ij}k_{\delta\delta}\right) \tag{45}$$

where $k_{ij} = {k_{ij}}^{+} - {k_{ij}}^{-}$, represents the change in extrinsic curvature across a hypothetical shell or surface. Here subscripts '+` and '_` corresponds to the outside and inside the shell respectively and k_{ij} is the extrinsic curvature tensor and k_{ij} provide the jump or discontinuity in the second fundamental form across the thin shell.

The extrinsic curvature in the 2nd fundamental form on each side of the shell are given by

$$ {k_{ij}}^{\pm} = -{\eta_{\gamma}}^{\pm}\left[\frac{\partial^2 x^{\gamma}}{\partial\emptyset^i\partial\emptyset^j} + \Gamma^{\gamma}_{\alpha\beta}\frac{\partial x^{\alpha}\partial x^{\beta}}{\partial\emptyset^i\partial\emptyset^j}\right]_{\Sigma} \tag{46}$$

where $\emptyset^i$ are the shell intrinsic co-ordinates ${\eta_{\gamma}}^{\pm}$ are normal vector to the surface $\sum$ and for the shape of spherically symmetric static metric.

$$ds^2 = f(r)dt^2 - \frac{dr^2}{f(r)} - r^2(d\theta^2 + \sin^2\theta\, d\emptyset^2) \tag{47}$$

The normal vector ${\eta_{\gamma}}^{\pm}$ can be written as:

$$ {\eta_{\gamma}}^{\pm} = \pm\left[g^{\alpha\beta}\frac{\partial f}{\partial x^{\alpha}}\frac{\partial f}{\partial x^{\beta}}\right]^{-\frac{1}{2}}\frac{\partial f}{\partial x^{\gamma}} \tag{48}$$

with $\eta^{\gamma}\eta_{\gamma} = 1$.

By using the Lanczos equation, the surface energy tensor $S_{ij} = dia[\sigma, -\nu, -\nu, -\nu]$ where σ is the surface energy density ϑ is the surface pressure.

The surface density σ can be obtained as:

$$\sigma = -\frac{1}{4\pi R_1}\left[\sqrt{f}\right]_{-}^{+}$$

which yields,

$$\sigma = -\frac{1}{4\pi R_1}\left[\sqrt{1 - \frac{2M}{R_1}} - \sqrt{1 - \frac{\left(8\pi + \frac{3}{2}\lambda_1 + 3\lambda_2\right)}{3}{R_1}^2\rho_k}\right] \tag{49}$$

and we obtain the surface pressure as:

$$\nu = -\frac{\sigma}{2} + \frac{1}{16\pi}\left[\frac{f'}{\sqrt{f}}\right]_{-}^{+}$$

which yields

$$\nu = \frac{1}{8\pi R_1}\sqrt{1 - \frac{2M}{R_1}} - \sqrt{1 - \frac{\left(8\pi + \frac{3}{2}\lambda_1 + 3\lambda_2\right){R_1}^2\rho_k}{3}} + \frac{1}{16\pi}\left[\frac{\frac{2M}{{R_1}^2}}{\sqrt{1 - \frac{2M}{R_1}}} + \frac{2\left(8\pi + \frac{3}{2}\lambda_1 + 3\lambda_2\right)R_1\rho_k}{\sqrt{1 - \frac{\left(8\pi + \frac{3}{2}\lambda_1 + 3\lambda_2\right){R_1}^2\rho_k}{3}}}\right] \tag{50}$$

By using equations (49) and (50), the equation of state parameter ω is given by

$$\omega(R_1) = \frac{\nu}{\sigma} = -\frac{1}{2} - \frac{R_1}{4}\frac{\frac{\frac{2M}{{R_1}^2}}{\sqrt{1 - \frac{2M}{R_1}}} + \frac{2\left(8\pi + \frac{3}{2}\lambda_1 + 3\lambda_2\right)R_1\rho_k}{\sqrt{1 - \frac{\left(8\pi + \frac{3}{2}\lambda_1 + 3\lambda_2\right){R_1}^2\rho_k}{3}}}}{\sqrt{1 - \frac{2M}{R_1}} - \sqrt{1 - \frac{\left(8\pi + \frac{3}{2}\lambda_1 + 3\lambda_2\right){R_1}^2\rho_k}{3}}} \tag{51}$$

Using the small parameter approximation $\frac{2M}{R_1} < 1$ and as well as $\frac{\left(8\pi + \frac{3}{2}\lambda_1 + 3\lambda_2\right){R_1}^2\rho_k}{3} << 1$ for real solutions and using binomial expansion of square root and keeping only first order terms, the equation (51) can be reduced as:

$$\omega(R_1) \approx -\frac{1}{2} + \frac{\frac{M}{R_1} + \frac{\rho_k\left(8\pi + \frac{3}{2}\lambda_1 + 3\lambda_2\right){R_1}^2}{3}}{\frac{\rho_k\left(8\pi + \frac{3}{2}\lambda_1 + 3\lambda_2\right){R_1}^2}{3} - \frac{3M}{R_1}} \tag{52}$$

The mass of the thin shell can be obtained as:

$$m_s = -4\pi {R_1}^2\sigma$$
$$= R_1\left[\sqrt{1 - \frac{\left(8\pi + \frac{3}{2}\lambda_1 + 3\lambda_2\right){R_1}^2\rho_k}{3}} - \sqrt{1 - \frac{2M}{R_1}}\right] \tag{53}$$

From equation (53), the overall mass M of Gravastar can be obtained as:

$$M = \frac{R_1}{2}\frac{\left(8\pi + \frac{3}{2}\lambda_1 + 3\lambda_2\right){R_1}^2\rho_k}{3} + m_s\sqrt{1 - \frac{\left(8\pi+\frac{3}{2}\lambda_1+3\lambda_2\right){R_1}^2\rho_k}{3}} - \frac{{m_s}^2}{2R_1} \quad (54)$$

Equation (54) can be written as:

$$M = \frac{R_1}{2}A + m_s\sqrt{1-A} - \frac{{m_s}^2}{2R_1} \quad (55)$$

where $A = \frac{\left(8\pi+\frac{3}{2}\lambda_1+3\lambda_2\right){R_1}^2\rho_k}{3}$.

From equation (55), we observed that the total Gravastar mass M is composed of physically distinct contributions from three regions. The term $\frac{R_1}{2}A$ represents the effective mass generated by the interior (core) region. The interior region between an effective vacuum energy region whose gravitational influenced depends on coupling parameters λ_1 and λ_2. The second term corresponds to the contribution of the thin shell region. The $\sqrt{1-A}$ can be interpreted as a gravitational redshift factor caused by the curvature of spacetime generated by the interior region. The effective contribution of this thin shell is reduced due to gravitational redshift effect. In case the parameter $A \to 1$, the shell contribution vanishes which indicates the formation of ultra-compact configuration approaching horizon formation. The third term $-\frac{{m_s}^2}{2R_1}$ represents the gravitational binding energy associated with the thin shell and reduces the total mass of the configuration, reflecting the energy required to assemble the shell against the own gravitational attraction.

In case $\lambda_1 = \lambda_2 = 0$, the expression reduces to GR which confirms the consistency of the model.

7. Conclusion

In this paper, we have investigated the Gravastar configuration introduced by [1,2] within the framework of modified gravity $f(R, L_m, T)$ gravity defined by the linear model $f(R, L_m, T) = R + \lambda_1 L_m + \lambda_2 T$ Gravastar model is an alternative to the Black Hole to avoid event horizon and central singularity. In this paper, we analyse the three regions of Gravastar with distinct equations of state (EOS) namely the interior region with the EOS $p = \rho$ and the vacuum exterior region resemble with schwarzchild solution with EOS $p = \rho = 0$.

In the interior region $(\omega = -1)$ $(0 \le r < R_{1)}$, the metric potential exhibits a regular and monotonically decreasing profile, indicating a non-singular de-Sitter type interior supported by constant energy density. The presence of coupling parameters λ_1 and λ_2 significantly influences the curvature behavior, thereby affecting the size and stability of the Gavastar configuration.

From fig 1, we notice that the metric potential $e^{-\lambda(r)}$ is monotonically decreasing with radial distance which indicates the increase of gravitational curvature. It starts from unity at the center which ensures regular and non-singular interior geometry. The function $e^{-\lambda(r)}$ vanishes at a finite limit which determines the effective boundary of the compact object. These conditions are consistent with physically viable Gravastar models in modified gravity.

In the intermediate thin shell region with the EOS equation $p = \rho$, the stiff matter layer provides pressure support that presents gravitational collapse and acts as a stabilizing layer separating the interior vacuum region from the exterior vacuum spacetime.

Fig 2 shows that as r increases the pressure approaches zero at the outer boundary of the shell which indicates a stable transition towards the exterior vacuum region.

The appropriate shell thickness is depend not only by the co-ordinate separation ϵ but also by the spacetime curvature given by the denominator of equation (40). The finite and small thickness of shell approximation ensures a stable, non-singular Gravastar configuration.

And we noticed that Gravastar's energy density depends on the radial co-ordinate r in the thin shell region.

In a Gravastar, entropy is entirely confined to the thin shell region where the matter obeys a stiff fluid equation of state. The interior and exterior regions of Gravastar contribute no entropy distinguishing Gravastar from black hole.

The junction conditions discussed in this paper ensure the smooth matching of the interior de-Sitter region to the exterior schwarzchild spacetime, while the metric coefficients are continuous at the junction surface, the discontinuity in extrinsic curvature gives rise to surface stresses, which physically represent the thin shell separating the two regions. The equation of state so obtained in this paper indicates that the thin shell of the Gravastar is composed of exotic matter characterized by negative pressure and the presence of the modified gravity coupling parameters λ_1 and λ_2 significantly alters the balance between gravitational attraction and repulsive effects. A stable Gravastar configurations, without the formation of an event horizon can be achieved through the domination of repulsive contributions arising from suitably chosen of coupling parameters.

The total Gravastar mass M is composed of three distinct contributions: Interior core contribution, thin shell contribution and the gravitational binding energy term. Thus the Gravastar model in $f(R, L_m, T)$ gravity, discussed in this paper preserve the essential features of Gravastar structure, originally proposed by Mazur and Mottola.

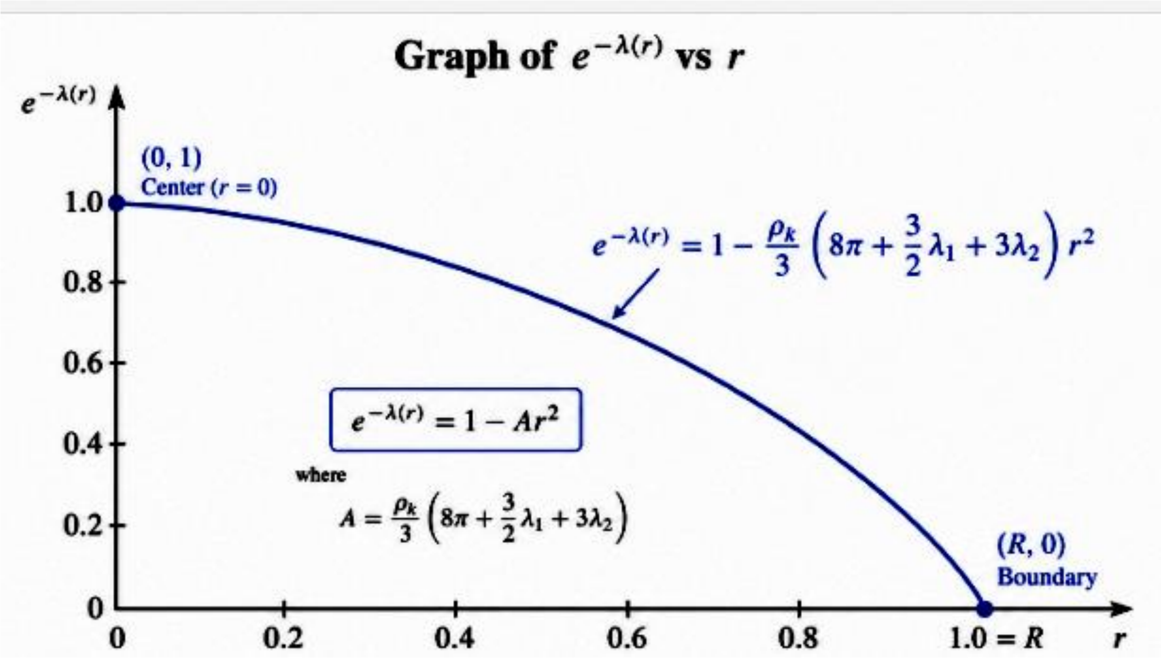

Figure 1: Plot of metric coefficient $e^{-\lambda}$ with respect to radial co-ordinate r in the interior of the Gravastar.

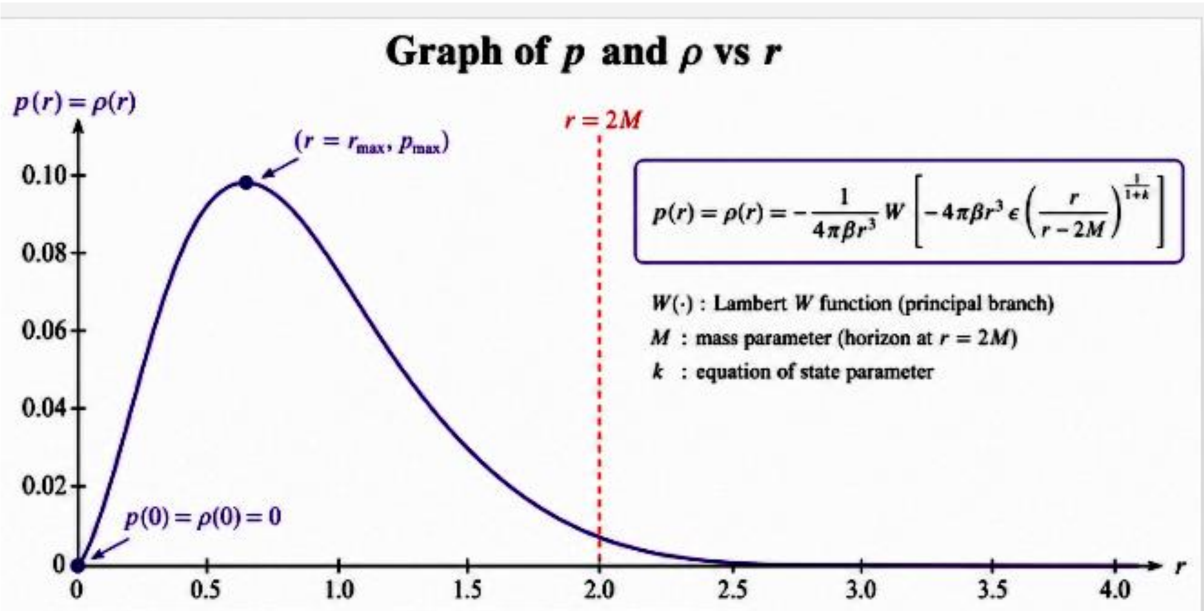

Figure 2: Plot of pressure p with respect to radial co-ordinate r of the ultrarelativistic fluid inside the thin shell of Gravastar.

Authors' contributions

The author read and approved the final manuscript.

Conflicts of interest

The author declares no conflict of interest.

Funding

This research received no external funding.

Data availability

No new data were created.

References

[1] P.O. Mazur, E. Mottola, Report number LA-UR-01-5067 (2001), arXiv/0109035 (2001).

[2] P.O. Mazur, E. Mottola, Gravitational condensate stars: An alternative to black holes, *Proc. Natl. Acad. Sci. U.S.A.* **101** (2004) 9545–9550.

[3] M.F. Shamir, S. Zia, Traversable gravastars in modified gravity, *Can. J. Phys.* **98** (2020) 849–856.

[4] T. Kubo, N. Sakai, Thin-shell gravastars in higher-dimensional Einstein gravity, *Phys. Rev. D* **93** (2016) 084051.

[5] R. Chan, M.F.A. da Silva, P. Rocha, A. Wang, Stable dark energy stars, *AIP Conf. Proc.* **1241** (2010) 571–576.

[6] S. Banerjee, S. Ghosh, N. Paul, F. Rahaman, Charged gravastar admitting conformal motion, *Eur. Phys. J. Plus* **135** (2020) 185.

[7] S. Ghosh, A. Kanjilal, A. Das, M. Houndjo, I.G. Salako, S. Roy, Gravastars in modified gravity theories, *Int. J. Mod. Phys. A* **35** (2020) 2050017.

[8] F.S. Lobo, R. Garattini, Self-sustained traversable wormholes in modified gravity, *J. High Energy Phys.* **2013** (2013) 065.

[9] P. Bhar, Gravastar models in modified gravity, *Astrophys. Space Sci.* **345** (2014) 457–464.

[10] F. Rahaman, S. Chakraborty, S. Ray, A.A. Usmani, S. Islam, Charged gravastars admitting conformal motion, *Int. J. Theor. Phys*. **54** (2015) 50–60.

[11] S. Perlmutter, et al. (Supernova Cosmology Project Collaboration), Measurements of Ω and Λ from 42 high-redshift supernovae, *Astrophys. J*. **517** (1999) 565–586, arXiv/9812133.

[12] A.G. Riess, et al. (Supernova Search Team Collaboration), Observational evidence from supernovae for an accelerating universe and a cosmological constant, *Astron. J*. **116** (1998) 1009–1038, arXiv/9805201.

[13] D.N. Spergel, et al. (WMAP Collaboration), Wilkinson Microwave Anisotropy Probe (WMAP) three-year results: Implications for cosmology, *Astrophys. J. Suppl. Ser*. **170** (2007) 377–408, arXiv/0603449.

[14] J. Dunkley, et al. (WMAP Collaboration), Five-year Wilkinson Microwave Anisotropy Probe observations: Likelihoods and parameters from the WMAP data, *Astrophys. J. Suppl. Ser*. **180** (2009) 306–329, arXiv:0803.0586 [astro-ph].

[15] D.J. Eisenstein, et al. (SDSS Collaboration), Detection of the baryon acoustic peak in the large-scale correlation function of SDSS luminous red galaxies, *Astrophys. J*. **633** (2005) 560–574, arXiv/0501171.

[16] T. Chiba, f(R) gravity and scalar-tensor gravity, *Phys. Lett. B* **575** (2003) 1–3.

[17] S. Nojiri, S.D. Odintsov, Modified f(R) gravity consistent with realistic cosmology: From matter dominated epoch to dark energy universe, *Phys. Lett. B* **657** (2007) 238–245.

[18] T. Harko, F.S.N. Lobo, S. Nojiri, S.D. Odintsov, f(R,T) gravity, *Phys. Rev. D* **84** (2011) 024020.

[19] T. Harko, F.S.N. Lobo, f(R,Lm) gravity, *Eur. Phys. J. C* **70** (2010) 373–379.

[20] T. Harko, et al., f(R,Lm,T) gravity, *Eur. Phys. J. C* **74** (2014) 2874.

[21] Z. Haghani, T. Harko, Generalizing the coupling between geometry and matter: f(R,Lm,T) gravity, *Eur. Phys. J. C* **81** (2021) 615.

[22] P. Bhar, P. Rej, Stable and self-consistent charged gravastar model within the framework of f(R,T) gravity, arXiv:2108.06989 [gr-qc] (2021).

[23] M. Sinha, S.S. Singh, Gravastar model in the framework of f(R,Lm,T) gravity, unpublished manuscript.

[24] Y.B. Zel'dovich, A hypothesis unifying the structure and entropy of the universe, *Mon. Not. R. Astron. Soc*. **160** (1972) 1P–3P.

[25] W. Israel, Singular hypersurfaces and thin shells in general relativity, *Nuovo Cimento B* **44** (1966) 1–14; *Erratum*, *Nuovo Cimento B* **48** (1967) 463.

[26] G. Darmois, Les équations de la gravitation einsteinienne, Mémorial des Sciences Mathématiques, Fascicule XXV, Gauthier-Villars, Paris (1927), Chap. V.

[27] K. Lanczos, Flächenhafte Verteilung der Materie in der Einsteinschen Gravitationstheorie, *Ann. Phys*. (Berlin) **379** (1924) 518–540.

[28] N. Sen, Über die Grenzbedingungen des Schwerefeldes an unstetigen Übergangsflächen, *Ann. Phys*. (Berlin) **378** (1924) 365–396.